The Amplification of Sinusoidal Signal by the Ramey's Magnetic Amplifier (Part I)

The Amplification of Sinusoidal Signal by the Ramey's Magnetic Amplifier (Part I)

Tsutomu TOKUDA*, Shiro HATA* and Yoshinao TAKASHIMA*

(Received February 10, 1958)

Abstract

In this paper, the characteristics of the Ramey's fast response magnetic amplifier circuit obtained by means of Fourier series as an amplifier of various sinusoidal low frequency signal are described. It is concluded that the Ramey's circuit is available as a linear amplifier of low frequency signal which is lower than $1/6$ of the source frequency.

1. Introduction

At present, with the development of the automation, the application of the magnetic amplifier in this field is increasing from day to day and many theoretical studies being attemped.

Already, authers had a report of the characteristics of the self saturable magnetic amplifier in the case of amplifying various sinusoidal signal[1]. At that time, we analyzed the magnetic amplifier output for the various sinusoidal low frequency input by means of Fourier analysis and showed the possibility of the linear amplification and the limit of signal frequency be able to amplify.

In this paper, the analytical results of the characteristics of the Ramey's fast response magnetic amplifier obtained by the same method as above mentioned are described.

2. Ramey's Fast Response Magnetic Amplifier

Fig. 2.1 (a) shows a schematic diagram of Ramey's circuit. The source voltage e_1 and e_2 are given as follows, $e_1 = E_1 \sin \omega t$, $e_2 = E_2 \sin \omega t$ respectively.

N_1 and N_2 are the number of turns of two reactor windings on an ideal core of which magnetic characteristic is shown in Fig. 2.1 (b). REC_1 and REC_2 are metalic rectifier with ideal characteristics.

When no signal voltage applied to the a–b terminals, the flux level in the core swings

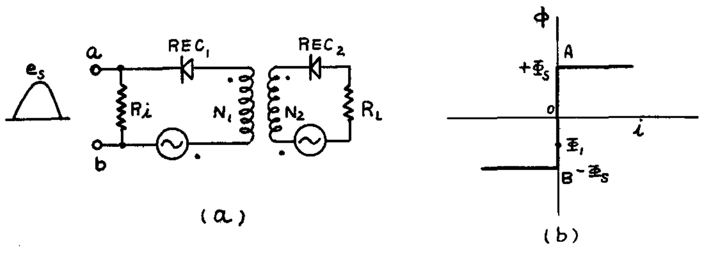

Fig. 2.1. Basic circuit of Ramey's magnetic amplifier.

* Department of Electrical Engineering, College of Engineering.

from the point A to B or B to A in Fig. 2.1 (b). For this condition, it is necessary to be satisfied the next relation.

$$\frac{E_1}{\omega N_1}=\frac{E_2}{\omega N_2}=\Phi_s\,. \tag{2.1}$$

Where Φ_s desinates the saturation flux in core.

Now, positive half cycle of a sinusoidal signal

$$e_s = E_s \sin \omega t \tag{2.2}$$
$$\begin{pmatrix} 2n\pi \leqq \omega t \leqq (2n+1)\pi \\ n=0,1,2,\cdots \end{pmatrix}$$

is applied to the a-b terminals. During $0 \leqq \omega t \leqq \pi$, source voltage e_2 is blocked by REC_2 and the core is excited by the voltage (e_1-e_s) from the side of N_1.

In this half cycle the core's flux level resets from the saturation point A and reaches Φ_1. This reset value is

$$\frac{1}{\omega N_1}\int_0^{\pi}(E_1-E_s)\sin\theta\, d\theta\,. \tag{2.3}$$

During the next half cycle, no signal voltage appears to the a-b terminals and the source voltage e_1 is blocked by REC_1. In N_2 side, the core flux is excited by the source voltage e_2 and flux level increases from Φ_1 to the point A. During $0 \leqq \omega t \leqq \theta_f$ in this half cycle, the flux level changes by the fallowing value,

$$\frac{1}{\omega N_2}\int_0^{\theta_f} E_s \sin\theta\, d\theta\,. \tag{2.4}$$

When the value of (2.4) grows into the reset value in the previous half cycle, the flux level reaches the point A and the reactor winding loses their reactance, consequently source voltage e_2 is impressed to the load resistance R_L only.

Because of the equality of the each flux level change during two adjacent half cycle, the next relations are yielded. They are

$$\frac{1}{\omega N_1}\int_0^{\pi}(E_1-E_s)\sin\theta\, d\theta=\frac{1}{\omega N_2}\int_0^{\theta_f} E_2 \sin\theta\, d\theta \tag{2.5}$$

$$\frac{1}{\omega N_1}\int_0^{\pi}E_s\sin\theta\, d\theta=\frac{1}{\omega N_2}\int_{\theta_f}^{\pi} E_2 \sin\theta\, d\theta\,. \tag{2.6}$$

The relation shown by (2.1), (2.5) and (2.6) means that in Fig. 2.2 the curve e_1/N_1 and e_2/N_2 are represented by a sine wave and obviously equal area in each half cycle and the hatched portions of the each half cycle possess equal area.

When $E_s=E_1$, the hatched portion possesses no area, consequently $\theta_f=0$ and with decreasing of E_s, the hatched portion area increases, finally θ_f grows into π when $E_s=0$. Thus, the voltage applied to R_L is changed by the variation of E_s.

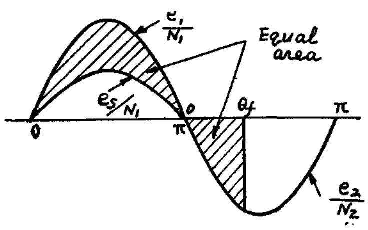

Fig. 2.2. Volt-second integral area by sinusoidal input.

Since this circuit operats by input voltage applied to the a-b terminals, the input impedance is higher than the ordinary magnetic amplifier circuit which operates with current, moreover, the response time of the output voltage to the input voltage is less than 1½ half cycle of source voltage.

3. The Static Characteristics of Ramey's Circuit

The Output vs. D-C Input Characteristics; When d-c voltage C is impressed to the a-b terminals in Fig. 2.1 the following relation is formed for the changed flux which is produced N_1 and N_2 winding during the adjacent two half cycles.

It is

$$\frac{1}{\omega N_1}\int_{\alpha}^{\beta}(E_1 \sin\theta - C)d\theta = \frac{1}{\omega N_2}\int_{0}^{\theta_f} E_2 \sin\theta\, d\theta\,. \tag{3.1}$$

Where α and β are the such phase angle as shown in Fig. 3.1.

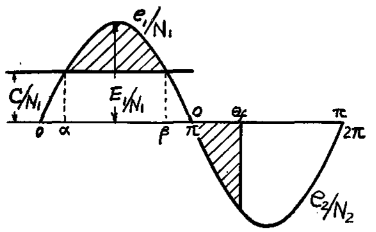

Fig. 3.1. Volt-second integral area by d-c input.

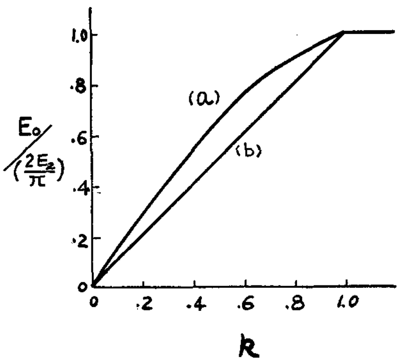

Fig. 3.2. Thoretical output vs. input characteristics.
(a) d-c input, (b) sinusoidal input.

Putting

$$C = kE_1\,, \quad (0 \leqq k \leqq 1) \tag{3.2}$$

obviously

$$\sin\alpha = \sin\beta = C/E_1 = k\,. \tag{3.3}$$

From (3.1), (3.2) and (3.3) we obtaine the next relation

$$\cos\theta_f = 1 - 2\sqrt{1-k^2} + k\pi - 2k\sin^{-1}k\,. \tag{3.4}$$

The mean value of output voltage E_0 of a half cycle is

$$E_0 = \frac{E_2}{\pi}(1 + \cos\theta_f)\,. \tag{3.5}$$

Substituting (3.4) for $\cos\theta_f$ in (3.5) we get E_0 as a function of k which varies with d-c voltage C as follows.

$$E_0 = \frac{2E_2}{\pi}\left(1 - \sqrt{1-k^2} + \frac{k\pi}{2} - k\sin^{-1}k\right)\,. \tag{3.6}$$

Giving various values to k, E_0 is calculated from (3.6). E_0 vs. k characteristics for the d-c input is shown by the curve (a) in Fig. 3.2.

The Characteristics of the Output vs. Input with Source Frequency; When the voltage presented in (2.2) is applied to the a-b terminals in Fig. 2.1, the relations of (2.5) and (2.6) exist. When the firing angle is θ_f, the mean output voltage E_0 is given as the following.

$$E_0 = \frac{1}{\pi}\int_{\theta_f}^{\pi} E_2 \sin\theta\, d\theta\,. \tag{3.7}$$

From (3.6) and (3.7) results

$$E_0 = \frac{2N_2}{\pi N_1} E_s = \frac{E_2}{\pi}(1 + \cos\theta_f) \tag{3.8}$$

and (3.8) shows that the output voltage E_0 is proportional to the amplitude E_s of the signal voltage e_s. The curve (b) in Fig. 3.2 shows this relation.

Moreover, from (2.5) the next relation is given.

$$\frac{2}{N_1}(E_1 - E_s) = \frac{E_2}{N_2}(1 - \cos\theta_f)\,. \tag{3.9}$$

4. The Amplication of Various Sinusoidal Low Frequency Signal

The amplification of the signal by the Ramey's circuit is possible when a d-c or very low frequency signal voltage is applied to the input terminals. However, as mentioned previously, there exists a linear relation between the input and output voltage only when tne input is an a-c voltage with source frequency. Therefore, in this paper, the characteristics in case that the input voltage to the Ramey's circuit terminals is an amplitude modulated wave are described. This amplitude modulated wave has the same frequency and phase as the source voltage e_1 and its amplitude is modulated by a very low frequency sinusoidal signal which should be amplified.

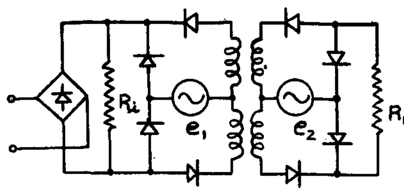

Fig. 4.1. Full wave Ramey's circuit.

For our experiment, two Ramey's circuit are combined to operate in all half cycle as shown in Fig. 4.1. Amplitude modulated input voltage previously mentioned is rectified by ring rectifier and impressed to the input terminal.

Fig. 4.2 show the wave form of the source voltage, the sinusoidal signal and the amplitude modulated voltage.

The sinusoidal voltage to be amplified e_i is given as the following.

$$e_i = \frac{E_1}{2}\sin\alpha t\,. \tag{4.1}$$

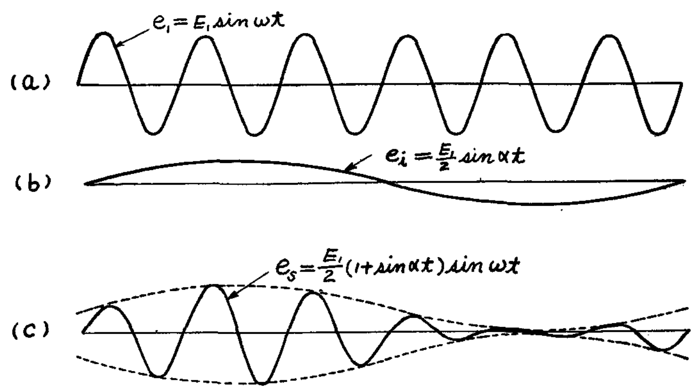

Fig. 4.2. (a) Source voltage wave form, (b) Sinusoidal signal, (c) Amplitude modulated wave.

Putting

$$\omega/\alpha = S \tag{4.2}$$

$$\omega t = \theta \tag{4.3}$$

the amplitude modulated wave with the sinusoidal signal is represented as the next.

$$e_s = \frac{E_1}{2}\left(1+\sin\frac{\theta}{S}\right)\sin\theta\,. \tag{4.4}$$

Two Ramey's circuit operate alternately in each half cycle and feed rectified voltage into the load resistance R_L as shown in Fig. 4.3 (b).

The amplitude of the pth half cycle of the amplitude modulated wave $E_{s,p}$ is given by the following formula.

$$E_{s,p} = \frac{E_1}{2}\left\{1+\sin\frac{(2p-1)\pi}{2S}\right\}. \tag{4.5}$$

By the substitution (4.5) in (3.8), the mean output voltage of $(p+1)$th half cycle $E_{0,p+1}$ is obtained.

$$\begin{aligned} E_{0,p+1} &= \frac{2N_2}{\pi N_1}E_{s,p} \\ &= \frac{2}{\pi}a\left\{1+\sin\frac{(2p-1)\pi}{2S}\right\} \end{aligned} \tag{4.6}$$

where

$$a = N_2/N_1\,. \tag{4.7}$$

Conveniently, θ_p desinates the firing angle in $(p+1)$th half cycle. θ_p is determined by the input voltage amplitude in pth half cycle. Moreover, for the condition that when $E_{s,p}=0$, $\theta_p=\pi$ and when $E_{s,p}=E_1$, $\theta_p=0$ the next relation must be satisfied.

$$\frac{E_1}{N_1} = \frac{E_2}{N_2}\,. \tag{4.8}$$

Using (3.9) and (4.8), we result (4.9) and (4.10) as follows.

$$\frac{2(E_1-E_{s,p})}{N_1} = \frac{E_2}{N_2}(1-\cos\theta_p) \tag{4.9}$$

$$\cos\theta_p = \frac{2E_{s,p}}{E_1}-1\,. \tag{4.10}$$

Combined (4.5) and (4.10), the firing angle θ_p is obtained

$$\cos\theta_p = \sin\frac{(2p-1)\pi}{2S}\,. \tag{4.11}$$

This formula gives the firing angle in $(p+1)$th half cycle in Fig. 4.2.

Since the right side of Eq. (4.11) is the value at $\theta=(2p-1)\pi/2$ in the function $\sin(\theta/S)$, the relation of Eq. (4.11) is shown as in Fig. 4.3 (a).

That is, as shown in Fig. 4.3 (b), we take as the origin the point 0 at $\theta=0$ of $\sin(\theta/S)$, and number each half cycle with symmetry at the origin through one period of the signal voltage as follows.

$$(-1,1)\ (-2,2)\ (-3,3)\cdots(-p,p)\cdots(-S,S)\,.$$

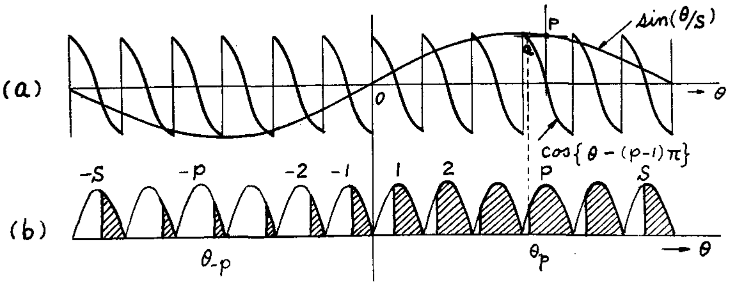

Fig. 4.3. (a) Graphical determination of firing angle.
(b) Output wave form through one period for sinusoidal input signal.

Drawing a perpendicular line to the phase axis at the middle point of pth half cycle, let across at the point P on the curve $\sin(\theta/S)$, and draw a parallel line to the phase axis through the point P. The phase of the cross point Q of this horizontal line and the curve $\cos\{\theta-(p-1)\pi\}$ in this half cycle gives the firing angle θ_p in the $(p+1)$th half cycle. Thus, repeating the above mentioned graphical proceduers, the firing angle in each half cycle through one period of the sinusoidal signal is obtained.

The hatched portion in Fig. 4.3 (b) shows the wave form of the instanteneous output voltage, where the firing angle in each half cycle is determined by above described procedures.

Because of the symmetry with the origin 0 of either $\sin(\theta/S)$ or $\cos[\theta-(p-1)\pi]$ in each half cycle, the next relation exists.

$$\theta_p+\theta_{-p}=\pi\,. \tag{4.12}$$

From Eq. (4.11), θ_p is obtained as follows.

$$\frac{(2p-1)\pi}{2S}=n\pi+(-1)^n\left(\frac{\pi}{2}-\theta_p\right) \tag{4.13}$$

where $n=1, 2, 3, \cdots$ (positive integer)

for $$p\leqq\frac{S+1}{2}$$

$$\theta_p=\frac{S-2p+1}{S}\cdot\frac{\pi}{2} \tag{4.14}$$

for $$\frac{S+1}{2}<p<\frac{2S+1}{2}$$

$$\theta_p=\frac{2p-S-1}{S}\cdot\frac{\pi}{2}\,. \tag{4.15}$$

Putting the instantenous output voltage $e_0(\theta)$, it is represented as follows.

$$e_0(\theta)=\frac{a_0}{2}+\sum_{n=1}^{\infty}\left(a_n\cos\frac{n}{S}\theta+b_n\sin\frac{n}{S}\theta\right) \tag{4.16}$$

where

$$a_n=\frac{1}{S\pi}\int_{-S\pi}^{S\pi}e_0(\theta)\cos\frac{n}{S}\theta\,d\theta \tag{4.17}$$

$$b_n=\frac{1}{S\pi}\int_{-S\pi}^{S\pi}e_0(\theta)\sin\frac{n}{S}\theta\,d\theta\,. \tag{4.18}$$

Giving the wave form shown by the hatched portion in Fig. 4.3 (b) to $e_0(\theta)$, Eq. (4.17), (4.18) become

$$a_n = \frac{1}{S\pi}\sum_{p=1}^{S}\left\{\int_{(p-1)\pi+\theta_p}^{p\pi}(-1)^{p-1}E_2\sin\theta\cos\frac{n}{S}\theta\,d\theta+\int_{-p\pi+\theta_{-p}}^{-(p-1)\pi}(-1)^{p}E_2\sin\theta\cos\frac{n}{S}\theta\,d\theta\right. \tag{4.19}$$

$$b_n = \frac{1}{S\pi}\sum_{p=1}^{S}\left\{\int_{(p-1)\pi+\theta_p}^{p\pi}(-1)^{p-1}E_2\sin\theta\sin\frac{n}{S}\theta\,d\theta+\int_{-p\pi+\theta_{-p}}^{-(p-1)\pi}(-1)^{p}E_2\sin\theta\sin\frac{n}{S}\theta\,d\theta\right. . \tag{4.20}$$

Applying the relation of (4.12) to (4.19) and (4.20), we have

$$a_n = 0\,,\qquad a_0 = 2E_2/\pi \tag{4.21}$$

when $n \neq S$

$$b_n = \frac{2E_2}{\pi}\frac{1}{S^2-n^2}\sum_{p=1}^{S}\left[S\cos\theta_p\sin\frac{n}{S}\{(p-1)\pi+\theta_p\}-n\sin\theta_p\cos\frac{n}{S}\{(p-1)\pi+\theta_p\}\right] \tag{4.22}$$

when $n = S$

$$b_s = \frac{E_2}{S}\left\{\frac{1}{2}\cdot\frac{1-\cos S\pi}{2}-\frac{1}{\pi}\sum_{p=1}^{S}(-1)^{p-1}(\theta_p-\cos\theta_p\sin\theta_p)\right\}. \tag{4.23}$$

Eq. (4.22) and (4.23) are identical with the result which was obtained by the calculation in the Ref. (2). Giving various value for S, we can obtaine the value of θ_p and harmonic component of signal frequency by means of tedious numerical calculations.

Though the formula by which obtain the value of θ_p is differ in case of this paper and the Ref. (2), it may be conclude analogically that the two system shown in this paper and in the Ref. (2) show same results by the reason of the characteristics shown in Fig. 3.2 (b) and Eq. (4.22) (4.23) are identical in two cases.

5. Conclusion

The analytical results of the characteristic obtained by the Ramey's magnetic amplifier circuit, when the amplitude modulated wave with same frequency as the source voltage is applied to the circuit, are described above.

Because of the necessity the amplitude modulating circuit, in above mentioned method needs some complex circuit. Though, when a sinusoidal low frequency signal is applied directly to the Ramey's circuit, the linearity of the characteristic does not exist as shown in Fig. 3.2 (a), the circuit is simple. But in this case it is difficult to obtaine the firing angle by calculation, so we must obtain it by graphycal method of which result we shall report in the future.

References

1) T. Tokuda and S. Hata: Lecture (No. 231) in Annual Meeting of I.E.E of Japan, Tokyo, May (1953).
2) K. Miyakoshi, S. Hata and S. Minamoto: J.I.E.E of Japan **74** 957 (1954).